Photophysik. Photo. Chem. **1950,** *45*, 222. (d) Adams, R.; Elslager, E. F.; Young, T. E. *J. Am. Chem. Soc.* **1953,** *75*, 663.
9. Craig, D. D.; Short, L. N. *J. Chem. Soc.* **1945,** 419.
10. Kim, T. R.; Chung, D. I.; Pyun, S. Y. *J. Korean Chem. Soc.* **1996,** *40*, 733.
11. (a) Cain, B. F.; Atwell, G. J. *J. Med. Chem.* **1968,** *11*, 295. (b) Cain, B. F.; AtWell, G. J.; Danney, W. A. *J. Med. Chem.* **1975,** *18*, 1110.
12. Koopman, H. *Rec. Trav.* **1961,** *80*, 1075.
13. Moloche, I.; Laidler, K. J. *J. Am. Chem. Soc.* **1951,** *73*, 1712.
14. AtWell, G. J.; Cain, B. F.; Seelye, R. N. *J. Med. Chem.* **1972,** *15*, 611.
15. Crossland, R. K.; Servis, R. L. *J. Org. Chem.* **1970,** *35*, 3195.
16. (a) Kharash, M.; Fuch, C. J. *J. Org. Chem.* **1948,** *23*, 97. (b) Hurd, C. D.; Geishbein, L. L: *J. Am. Chem. Soc.* **1947,** *69*, 2338.
17. Albert, A. *J. Chem. Soc.* **1965,** 4653.
18. Kim, T. R.; Crowell, T. I. *J. Am. Chem. Soc.* **1973,** *95*, 6781.
19. (a) Kim, T. R.; Huh, T. S.; Han, I. S. *Bull. Korean Chem. Soc.* **1982,** *3*, 162. (b) Kim, T. R.; Ryu, J. Y.; Ha, D. C. *J. Korean Chem. Soc.* **1988,** *32*, 260. (c) Kim, T. R.; Chung, Y. S.; Chung, M. S. *J. Korean Chem. Soc.* **1991,** *35*, 268.
20. From the value of k_1^{SH}=1.46 x 10^{-5} $M^{-1}sec^{-1}$, (k_1^{SH}/k_{-1}^{SH}) k_2^{H20}[H_2O]= 7.48 x $10^{-7}M^{-1}sec^{-1}$, (k_1^{SH}/k_{-1}^{SH}) k_2^{OH} = 4.43 x $10^{2}M^{-1}sec^{-1}$, [CH_3COO^-]=0.4 M, [OH^-]= 6.03 x 10^{-10} M and observed rate constant k_t, the value of catalytic constant of acetate ion (k_1^{SH}/k_1^{SH}) k_2^{OAc} can be determined and is found to be 1.50 x $10^{-5}M^{-1}sec^{-1}$, By substituting above data into equation (9), k_0 is given by the following equation (9-1).

$$\frac{1}{k_0} = \frac{1.65 \times 10^{-5} + 1.53 \times 10^{-4}[OAC^-]}{1.66 \times 10^{-11} + 2.37 \times 10^{-9}[OAC^-]} \quad (9\text{-}1)$$

As a result, over-all rate constant becomes;

$$k_t = 3.53 \times 10^{-4}[H_3O^+] + \frac{1.66 \times 10^{-11} + 2.37 \times 10^{-9}[OAC^-]}{1.65 \times 10^{-5} + 1.53 \times 10^{2}[OAC^-]} + 1.12 \times 10^{2}[OH^-] \quad (9\text{-}2)$$

Figure 3 shows that the values of over-all rate constant, k_t, calculated by equation (9-2) are in good agreement with observed values.

21. $$\frac{1}{k_0} = \frac{1}{k_1^{SH}} + \frac{1}{\left(\frac{k_1^{SH}}{k_{-1}^{SH}}\right)} \{k_1^{H2O}[H_2O] + k_2^{OH}[OH^-] + k_2^{B}[B^-]\} \quad (10)$$

From the value of k_1^{SH}= 1.46 x $10^{-5}M^{-1}sec^{-1}$, (k_1^{SH}/k_{-1}^{SH}) k_2^{H2O}[H2O]= 7.48 x $10^{-7}M^{-1}sec^{-1}$, (k_1^{SH}/k_{-1}^{SH}) k_2^{0H}= 4.43 x $10^{2}M^{-1}sec^{-1}$, [B^-]=1.25 x 10^{-4}M, [OH^-]=10^{-8} M and observed rate constant k_t, the value of catalytic constant of various general bases (k_1^{SH}/k_{-1}^{SH}) k_2^{B} can be determined.

Optimization of Synthetic Parameters for Mesoporous Molecular Sieve MCM-41 Using Surfactant CTACl

Dong Ho Park, Chi-Feng Cheng*, and Jacek Klinowski*

Department of Chemistry, Inje University, Kimhae, Kyongnam 621-749, Korea
**Department of Chemistry, University of Cambridge, Lensfield Road, Cambridge CB2 1E W, U. K.*
Received October 11, 1996

High quality MCM-41 is prepared from a gel of molar composition SiO_2: 0.20 CTACl: 0.18 TMAOH: 25 H_2O aged at 20 °C for 24 hours before crystallization lasting for 48 hours. The (110) and (200) peaks of XRD pattern of high quality MCM-41 are unusually well resolved and the FWHM (full-width-at-half-maximum) of the (100) peak is 0.13° for as-prepared MCM-41 and 0.21° for calcined one, which indicate well-developed crystals. The properties of the crystal depend on the source and concentration of the reactants and the gel aging time. There is no induction period in the course of the synthesis, which is conveniently monitored by pH measurement. Gel aging, during which a spatial distribution of silicate polyanions and micellar cations is established, is essential for preparing high quality MCM-41. Surfactants with the same cationic organic group but different counteranions change the crystallization behavior. Highly basic gel (pH=12.6) favours the lamellar product; the quality of MCM-41 is lower as insufficient TMAOH is available to dissolve the silica.

Introduction

Zeolite-based molecular sieves have a limited pore diameter and the known mesoporous materials such as silica gel, activated carbon and pillard clay have irregularly spaced pore with broad pore size distribution. There has been increasing demand for crystalline mesoporous molecular sieves with pores of uniform diameter. The synthesis of the mesoporous molecular sieve MCM-41 with one-dimensional channels 16-100 Å in diameter which allow fast diffusion

of large molecules has responded to this need.[1,2] The aggregates of a surfactant serve as the template[1~5] instead of single organic molecules as in the synthesis of conventional sieves. The high thermal and hydrothermal stability, uniform diameter and shape of the pores over micrometer length scales, as well as, the prospect of tuning the pore aperture make MCM-41 of interest to heterogeneous catalysis and molecular separation. The most important potential applications are the separation of proteins, the selective adsorption of large molecules from effluents and the processing of tar sand and high distillates of crude oils to valuable low-boiling products. With potential catalytic applications in mind, much attention has been given to isomorphous substitution of heteroelements into the silicate framework.[6~18]

The new material has been characterized in detail,[19~23] and different formation mechanisms have been proposed,[1~4,20,22,24~27] since Mobil group suggested the liquid-crystal templating mechanism initiated by the hexagonal array of cylindrical micelles, which is possibly mediated by the presence of silicated ions.[1,2] The synthesis, characterization and potential application of mesoporous materials was reviewed by A. Sayari.[28] Most applications require MCM-41 with a narrow pore size distribution, large surface area and long-range order. As the parameters affecting the synthesis of Si-MCM-41 have not been systematically studied, we have used XRD and magic-angle-spinning (MAS) NMR to understand the role of the source and concentration of the reactants, the gel aging time, the temperature and the duration of the crystallization using CTACl as a surfactant in the alkali metal-free media. The relative crystallinity of MCM-41 product was evaluated from the relative intensity and sharpness of the XRD peaks.

Experimental

Synthesis

The chemicals used in the synthesis were fumed silica (99.8%, metal-free, surface area=400 ± 20 m^2/g, Sigma), Cab-O-Sil M-5 fused silica (surface area=390 ± 40 m^2/g, BDH), cetyltrimethylammonium chloride (CTACl, 25 wt% aqueous solution, Aldrich) and tetramethylammonium hydroxide (TMAOH, 25 wt% aqueous solution, Sigma). Purely silicious MCM-41 was prepared as follows. TMAOH and CTACl were added to deionized water with stirring at room temperature until the solution became clear. The silica source was added to the solution with stirring and the gel was aged at 20 °C. The molar composition of final gel mixture was SiO_2: 0.10-0.50 CTACl: 0.14-0.22 TMAOH: 20-35 H_2O. The mixtures were reacted for 48 h at 150 °C in Teflon-lined stainless steel autoclaves. The aging time was varied. The product was filtered, washed with distilled water, dried in air at 60 °C and finally calcined at 550 °C for 8 h.

Sample Characterization

X-ray diffraction. XRD patterns were recorded using a Philips 1710 powder diffractometer with Cu Kα radiation (40 kV, 40 mA), 0.02° step size and 1 s step time.

Solid-state NMR. MAS NMR spectra were recorded at 9.4 T using a Chemagnetics CMX-400 spectrometer with zirconia rotors 7.5 mm in diameter spun in air at 4 kHz. ^{29}Si spectra were acquired at 79.4 MHz with 90° pulses and 600 s recycle delays; ^{13}C spectra at 100.6 MHz with 45° pulses and 5 s recycle delays and high-power proton decoupling. Chemical shifts are given in ppm from external tetramethylsilane (TMS).

Results and Dicussion

As the crystallization of highly silicious zeolites is accompanied by changes in pH, the monitoring of acidity is a simple way to follow the reaction.[29,30] As a results of the formation of the zeolitic framework (composed of ≡ SiOSi ≡ units) *via* the condensation reaction

$$\equiv SiO^- + HO\text{-}SiO \equiv \rightleftarrows \equiv SiOSi \equiv + OH^- \quad (1)$$

the pH abruptly increases during the nucleation period. However, this is not the case for MCM-41. Here, the pH decreases during crystallization of all samples, as shown in Table 1, because the dissolution of the neutral silica source drives the reaction (1) to the left. The charge of the silicate polyanions is balanced by the cationic micelle heads, and the formation of the ≡ SiOSi ≡ units proceeds largely *via*

Table 1. Chemical composition of the synthesis mixtures, pH values during synthesis and phase of as-prepared samples using XRD patterns

Sample name	Reaction gel composition (molar ratio)	pH initial	pH aged	pH final	Phase by XRD
MCM41-a1	SiO_2: 0.27CTACl: **0.22** TMAOH: 30H_2O	12.6	11.5	10.3	lamellar
MCM41-a2	SiO_2: 0.27CTACl: **0.20** TMAOH: 30H_2O	12.4	11.4	10.6	hexagonal
MCM41-a3	SiO_2: 0.27CTACl: **0.18** TMAOH: 30H_2O	12.3	11.3	10.5	hexagonal
MCM41-a4	SiO_2: 0.27CTACl: **0.16** TMAOH: 30H_2O	12.3	11.2	10.4	hexagonal
MCM41-a5	SiO_2: 0.27CTACl: **0.14** TMAOH: 30H_2O	12.1	11.1	10.2	hexagonal
MCM41-b1	SiO_2: **0.10** CTACl: 0.18TMAOH: 30H_2O	12.6	11.7	10.2	hexagonal
MCM41-b2	SiO_2: **0.20** CTACl: 0.18TMAOH: 30H_2O	12.5	11.4	10.1	hexagonal
MCM41-b3	SiO_2: **0.35** CTACl: 0.18TMAOH: 30H_2O	12.2	11.2	10.1	hexagonal
MCM41-b4	SiO_2: **0.50** CTACl: 0.18TMAOH: 30H_2O	12.1	11.1	10.1	hexagonal
MCM41-C1	SiO_2: 0.27CTACl: 0.18TMAOH: **20** H_2O	12.4	11.4	10.0	hexagonal
MCM41-C2	SiO_2: 0.27CTACl: 0.18TMAOH: **25** H_2O	12.4	11.4	10.2	hexagonal
MCM41-C3	SiO_2: 0.27CTACl: 0.18TMAOH: **35** H_2O	12.2	11.3	10.1	hexagonal

the reaction.

$$\equiv \text{Si-OH} + \text{HO-SiO} \equiv \rightleftarrows \equiv \text{SiOSi} \equiv + \text{H}_2\text{O} \quad (2)$$

As a result, the pH continues to decrease until *ca.* 10 during the nucleation and crystallization period, to stabilize only when crystallization is complete, as shown in Table 1.

The XRD pattern of MCM-41 prepared from Cab-O-Sil fumed silica is of much lower quality than when Sigma fumed silica is used (Figure 1). Both sources of silica have high surface areas but are manufactured differently. On the basis of the chemical shift in ^{29}Si MAS NMR spectra, the peak at -109 ppm has to be assigned to the $Si(OSi)_4(Q^4)$ sites. The $Si(OSi)_2(O^-M^+)_2$ and $Si(OSi)_3(O^-M^+)$ sites, where M^+ is the template cation, give peaks at approximately the same position as the $Si(OSi)_2(OH)_2(Q^2)$ and $Si(OSi)_3OH(Q^3)$ sites, that is at *ca.* -91 and -100 ppm, respectively.[31] The ^{29}Si MAS NMR spectra of the Sigma and Cab-O-Sil silicas with and without aging show that the proportion of Q^4 units in the former is slightly lower (Figure 2). The lower fraction of Q^4 units (corresponding to a lower degree of silica polymerization) in the aged (as opposed to non-aged) Sigma silica conforms that the silica is partially dissolved during aging. Aged Sigma silica contains a much lower fraction of Q^4 units than aged Cab-O-Sil silica. Thus the source of silica also affects the quality of the product.

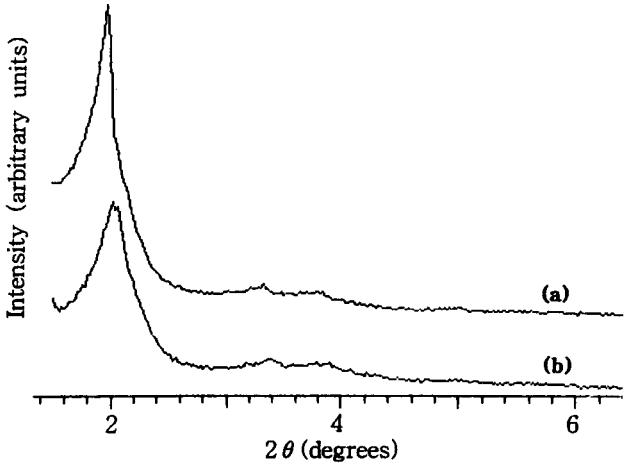

Figure 1. XRD patterns of MCM-41 synthesizes from a gel of SiO_2: 0.27CTACl: 0.18TMAOH: $30H_2O$ using different silica source; (a) Sigma fumed silica and (b) Cab-O-Sil fumed silica.

Figure 3 shows the crystallinity of Si-MCM-41 for different aging times from reaction gel composition of SiO_2: 0.27CTACl: 0.18TMAOH: $30H_2O$. The decrease of the pH at longer aging time (12.4, 11.9, and 11.3 for 0 h, 6 h, and 24 h, respectively) indicates that the OH^- ions are consumed to dissolve the silica source to form smaller silicate polyanions, to reverse the reaction (1). The product of no-aging synthesis have low crystallinity of hexagonal phase. As shown in Figure 3(a), (110) and (200) peaks of XRD pattern are not resolved by broadening due to low crystallinity. The crystallinity of the products increases with increasing aging time. After aging for 24 h, the pH stabilizes and the crystallinity of the product reaches a maximum under this synthetic condition and above reaction gel composition. Aging at 20 °C, during which some of the gel dissolves and a spatial arrangement of the silicate polyanions and micellar cations for hexagonal phase is partially established, is thus essential for preparing high quality MCM-41.

Crystallization of purely silicious zeolites normally in-

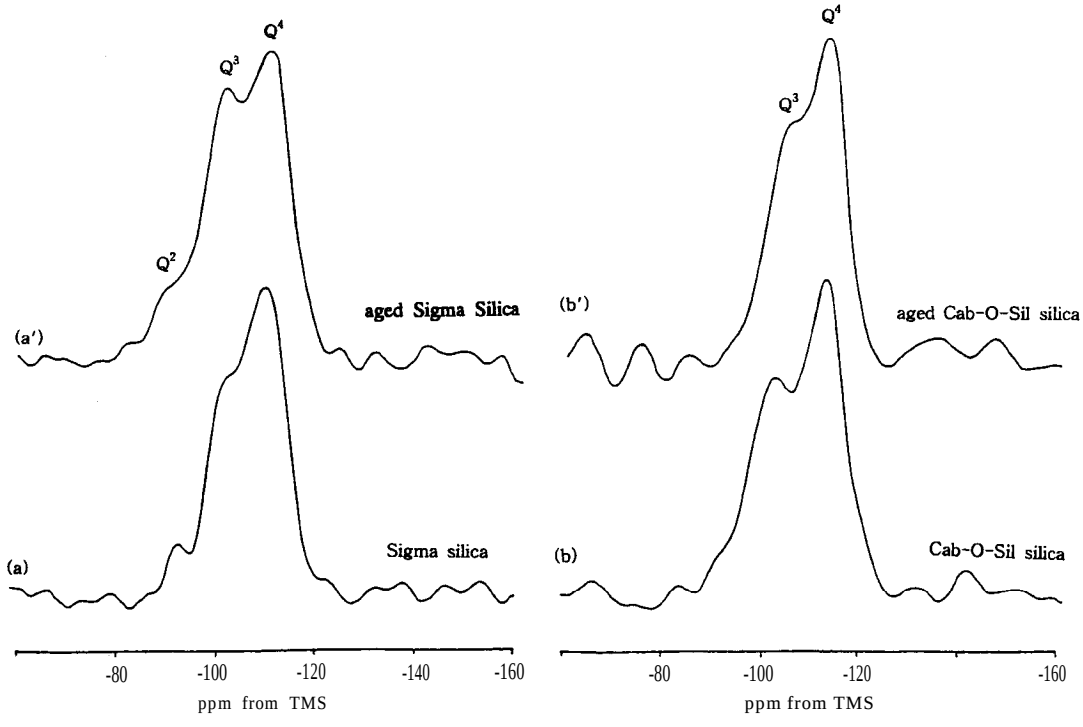

Figure 2. ^{29}Si MAS NMR spectra of Sigma fumed silica (a) no aging and (a') aging; Cab-O-Sil fumed silica (b) no aging and (b') aging for 24 h. The gel composition is the same as in Figure 8.

volves an induction period during which the silica source is dissolved to form small anionic silicate units (monomers, dimers, double 4-ring, etc.), which then undergo condensation.[32] However, no induction period is found in the course of the synthesis of MCM-41, because the high-molecular-weight silicate polyanions[20] formed during the aging period are needed to match the cationic charge of the surfactant micelles.

Figure 4 shows XRD patterns of MCM-41 prepared using different concentrations of TMAOH. The molar ratio of TMAOH to SiO_2 of gel was changed in the range of 0.22-0.14, as shown in Table 1. pH values of initial and aged gel

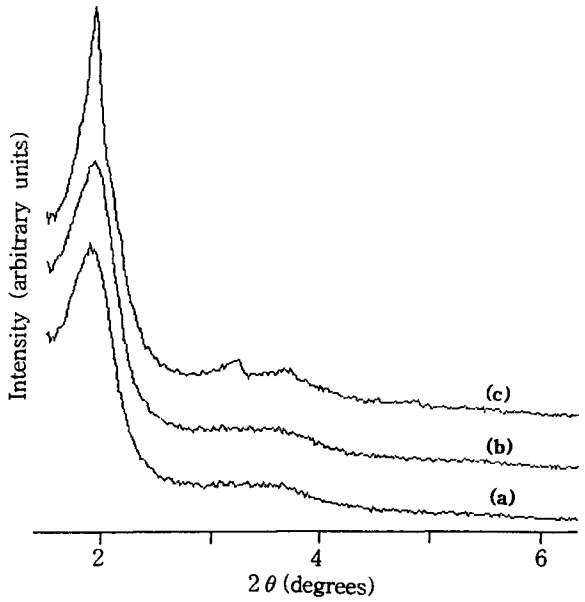

Figure 3. XRD Patterns of MCM-41 synthesized from a gel of SiO_2: 0.27CTACl:0.18TMAOH: $30H_2O$ after aging for (a) 0 h, (b) 6 h, and (c) 24 h.

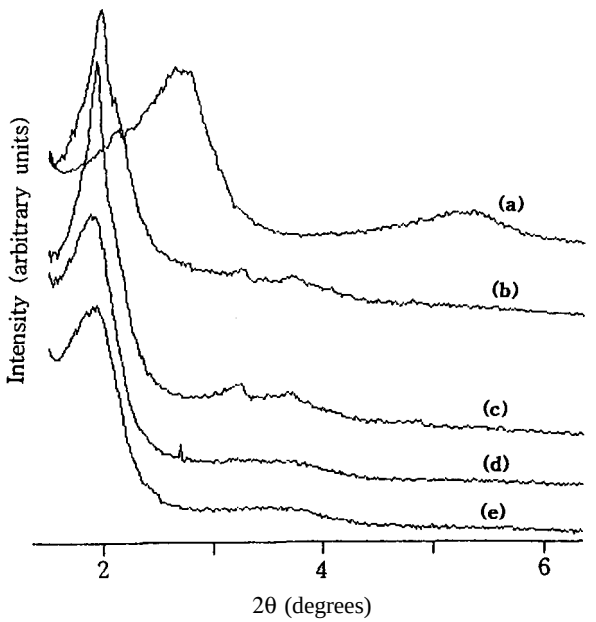

Figure 4. XRD patterns of (a) MCM41-a1, (b) MCM41-a2, (c) MCM41-a3, (d) MCM41-a4, and (e) MCM41-a5.

were decreased with TMAOH concentration. High quality of product is prepared from the gel of molar ratio TMAOH/SiO_2= 0.18. A higher concentration of TMAOH increases the content of the lamellar phase which turns amorphous upon calcination. The XRD pattern of MCM41-a1 indicates the formation of pure lamellar phase (Figure 4(a)). A lower concentration also gives a hexagonal phase of lower quality because the gel contains insufficient organic base to digest the silica.

Figure 5 shows the dependence of the quality of MCM-41 on the concentration of CTACl. The molar ratio of CTACl to SiO_2 of gel was changed in the range of 0.10-0.50, as shown in Table 1. High quality of product is prepared from CTACl/SiO_2= 0.20, which is nearly similar to the ratio that virtually all of the SiO_2 and CTA^+ take a participation in crystallization.[4] XRD pattern of MCM41-b1 (CTACl/SiO_2= 0.1) is less intense due to a surplus of silica but the resolution slightly better than that of MCM41-b2. With increasing the CTACl concentration above 0.20, the relative crystallinity evaluated from XRD peaks was decreased, which may be attributable to degrade the crystallinity of the product due to prohibition from growing of MCM-41 crystallite and decreased polymerization of silica by an excess of surfactant.

Figure 6 shows the dependence of the quality of MCM-41 on the concentration of water. High quality of product is prepared from H_2O/SiO_2= 25. XRD of MCM41-c1 shows a good resolution and high intensity resulted from highly crystalline MCM-41, but slightly broader than that of MCM41-c2. It may be due to lower water content not enough to make the reaction gel homogeneous. The dilution of other reagents in reaction gel by higher water concentration deteriorates the crystallinity.

High quality MCM-41 is prepared from a gel of molar composition SiO_2: 0.20CTACl : 0.18TMAOH: $25H_2O$ aged at 20 °C for 24 h before crystallization for 48 h at 150 °C.

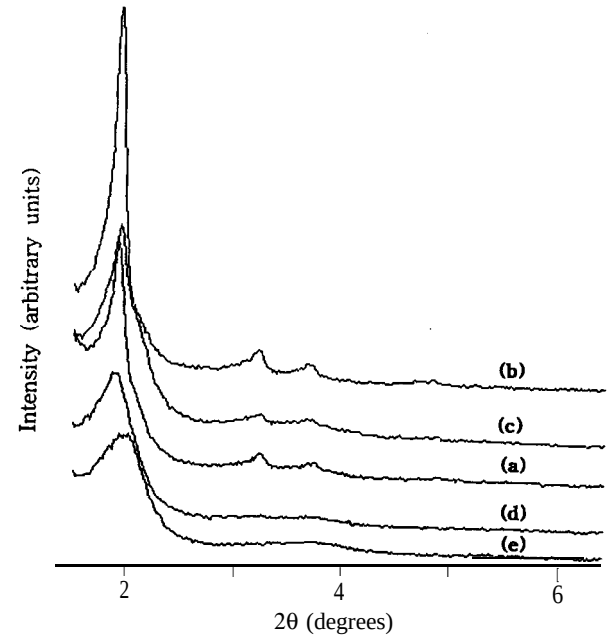

Figure 5. XRD patterns of (a) MCM41-b1, (b) MCM41-b2, (c) MCM41-a3, (d) MCM41-b3, and (e) MCM41-b4.

The pH value was 12.5, 11.4 and 10.2 for initial reaction mixture, aged one, and crystallized one, respectively. While this does not imply that better MCM-41 cannot form under other condition, the XRD patterns of purely silicious MCM-41 reflect the best quality of crystallite under all condition in the present study (Figure 7). The (110) and (200) peaks are unusually well resolved. The FWHM (full-width-at-half-maximum) of the (100) peak is 0.13° for as-prepared MCM-41 and 0.21° for calcined one. These indicate that the crystals are particularly well-developed.

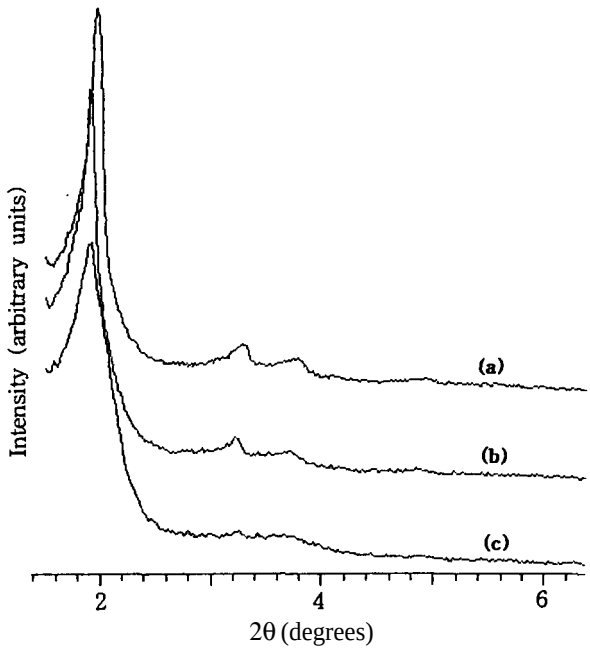

Figure 6. XRD patterns of (a) MCM41-c1, (b) MCM41-c2, and (c) MCM41-c3.

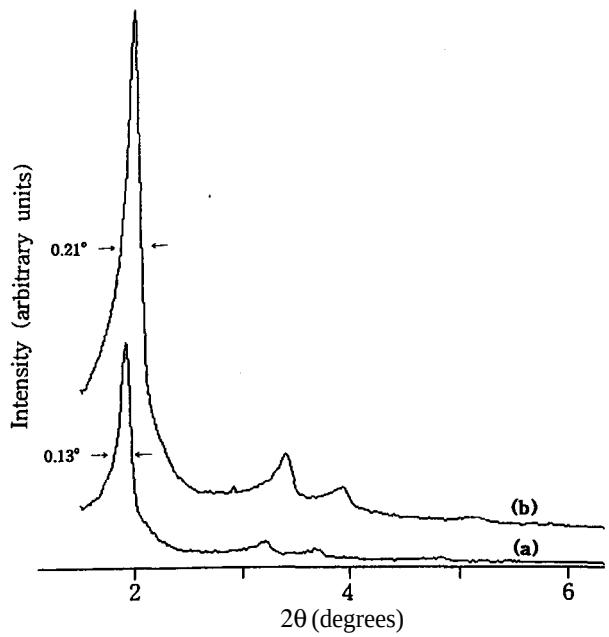

Figure 7. XRD patterns of (a) as-made and (b) calcined MCM-41 synthesized from a gel of SiO_2:0.20CTACl:0.18TMAOH: $25H_2O$ aged for 24 h and reacted at 150 °C for 48 h. Degrees in Figure indicate the full width at half maximum of (100) peak.

High quality MCM-41 using CTABr as a surfactant source was prepared from a gel of molar composition SiO_2: 0.27CTABr:0.19TMAOH:40H_2O, which XRD was illustrated in Figure 8. The difference of gel composition is attributable to the nature of the anionic species. At room temperature, the volubility of CTABr in water is less than 10% while that of CTACl exceeds 25%. The much higher solvation ability of CTACl is reflected in the ^{13}C NMR spectra of 7% aqueous solutions of CTACl and CTABr (Figure 9), in which both surfactants exist in the form of micelles. The spectral linewidth of peaks from CTABr(aq) is greater than that from CTACl(aq). The width of the ^{13}C line at *ca.*

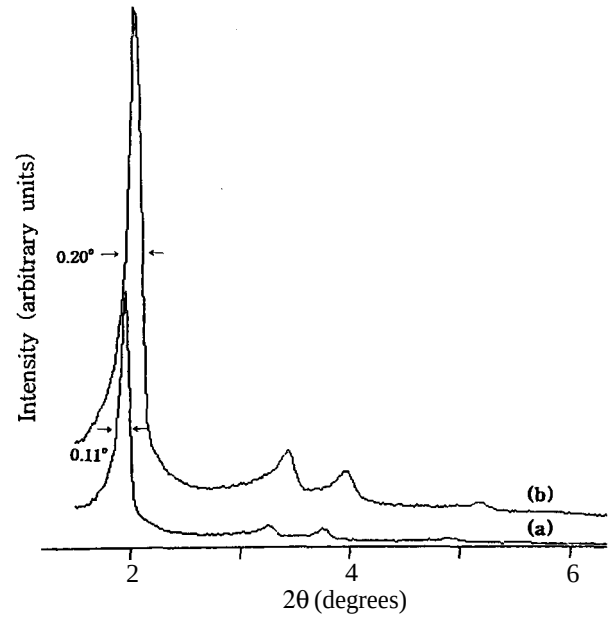

Figure 8. XRD patterns of (a) as-made and (b) calcined MCM-41 synthesized from a gel of SiO_2: 0.27CTABr : 0.19TMAOH : $40H_2O$ aged 24 h and reacted at 150 °C for 48 h. Degrees in figure indicate the full width at half maximum of (100) peak.

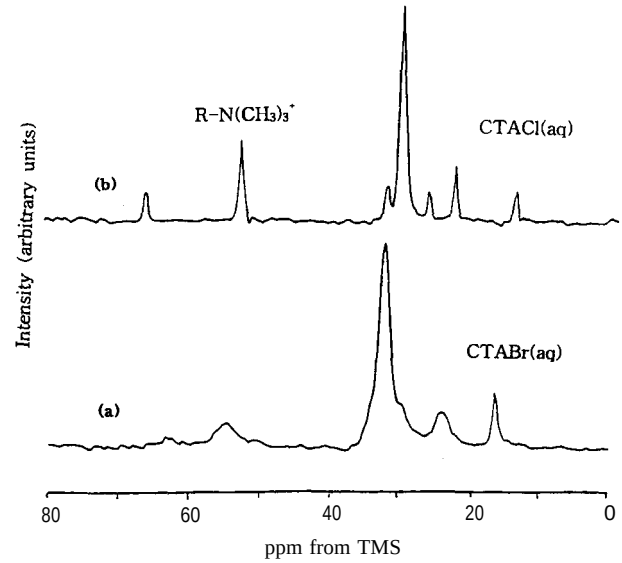

Figure 9. ^{13}C MAS NMR spectra with high-power proton decoupling of 7% aqueous solutions of (a) CTABr and (b) CTACl.

54 ppm from the methyl group bonded to the nitrogen of the micelle head in CTABr(aq) is 5 times greater, because the quadrupolar ^{79}Br and ^{81}Br anions are more difficult to solvate and interact more strongly with the cationic micelle head than $^{35}Cl^-$ and $^{37}Cl^-$ anions.

References

1. Kresge, C. T.; Leonowicz, M. E.; Roth, W. J.; Vartuli, J. C.; Beck, J. S. *Nature* **1992,** *359*, 710.
2. Beck, J. S.; Vartuli, J. C.; Roth, W. J.; Leonowicz, M. E.; Kresge, C. T.; Schmitt, K. D.; Chu, C. T.-W.; Olsen, D. H.; Sheppard, E. W.; McCullen, S. B.; Higgins, J. B.; Schlenker, J. L. *J. Am. Chem. Soc.* **1992,** *114*, 10834.
3. Chen, C.-Y.; Burkett, S. L.; Li, H.-X.; Davis, M. E. *Microporous Mater.* **1993,** *2*, 27.
4. Cheng, C.-F.; Luan, Z.; Klinowski, J. *Langmuir* **1995,** *11*, 2815.
5. Beck, J. S.; Vartuli, J. C.; Kennedy, G. J.; Kresge, C. T.; Roth, W. J.; Schramm, S. E. *Chem. Mater.* **1994,** *6*, 1816.
6. Luan, Z.; Cheng, C.-F.; Zhou, W.; Klinowski, J. *J. Phys. Chem.* **1995,** *99*, 1018.
7. Luan, Z.; Cheng, C.-F.; He, H.; Klinowski, J. *J. Phys. Chem.* **1995,** *99*, 10590.
8. Luan, Z.; He, H.; Zhou, W.; Cheng, C.-F.; Klinowski, J. *J. Chem. Soc., Faraday Trans.* **1995,** *91*, 2955.
9. Corma, A.; Navarro, M. T.; Perez-Pariente, J. *J. Chem. Soc., Chem. Commun.* **1994,** 147.
10. Tanev, P. T.; Chibwe, M.; Pinnavaia, T. J. *Nature* **1994,** *368*, 321.
11. Cheng, C.-F.; He, H.; Zhou, W.; Klinowski, J.; Sousa Goncalves, J. A.; Gladden, L. F. *J. Phys. Chem.* **1996,** *100*, 390.
12. Cheng, C.-F.; Alba, M. D.; Klinowski, *J. Chem. Phys. Lett.* (in press)
13. Reddy, K. M.; Moudrakovski, I. L.; Sayari, A. *J. Chem. Soc., Chem. Commun.* **1994,** 1059.
14. Sayari, A.; Danuman, C.; Moudrakovski, I. L. *Chem. Mater.* **1995,** *7*, 813.
15. Sayari, A.; Moudrakovski, I. L.; Danuman: C.; Ratcliffe, C. I.; Ripmeester, J. A.; Preston, K. F. *J. Phys. Chem.* **1995,** *99*, 16373.
16. Yuan, Z. Y.; Liu, S. Q.; Chen, C. H.; Wang, J. Z.; Li, H. X. *J. Chem. Soc., Chem. Commun.* **1995,** 973.
17. Zhao, D. Y.; Goldfarb, D. *J. Chem. Soc., Chem. Commun.* **1995,** 875.
18. Cheng, C.-F.; Klinowski, J. *J. Chem. Soc., Faraday Trans.* **1996,** *92*, 289.
19. Chen, C.-Y.; Li, H.-X.; Davis, M. E. *Microporous Mater.* **1993,** *2*, 17.
20. Monnier, A.; Schuth, F.; Hue, Q.; Kumar, D.; Margolese, D.; Maxwell, R. S.; Stucky, G. D.; Krishnamurty, M.; Petroff, P.; Firouzi, A.; Janicke, M.; Chmelka, B. F. *Science* **1993,** *261*, 1299.
21. Coustel, N.; Renzo, F. D.; Fajula, F. *J. Chem. Soc., Chem. Commun.* **1994,** 967.
22. Steel, A,; Carr, S. W.; Anderson, M. W. *J. Chem. Soc., Chem. Commun.* **1994,** 1571.
23. Ryoo, R.; Kim, J. M. *J. Chem. Soc., Chem. Commun.* **1995,** 711.
24. Cheng, C.-F.; He, H.; Zhou, W.; Klinowski, J. *Chem. Phys. Lett.* **1995,** *244*, 117.
25. Alfredsson, V.; Keung, M.; Monnier, A.; Stucky, G. D.; Unger, K. K.; Schuth, F. *J. Chem. Soc., Chem. Commun.* **1994,** 921.
26. Chenite, A.; Page, Y. L.; Sayari, A. *Chem. Mater.* **1995,** *7*, 1015.
27. Vartuli, J. C.; Kresge, C. T.; Leonowicz, M. E.; Chu, A. S.; McCullen, S. B.; Johnson, I. D.; Sheppard, E. W. *Chem. Mater.* **1994,** *6*, 2070.
28. Sayari, A In *Studies in Surface Science and Catalysis;* Chon, H. *et al.*, Eds.; Elsevier: Amsterdam, Netherlands, 1996; Vol. 102, p 1.
29. Casci, J. L.; Lowe, B. M. *Zeolites* **1983,** *3*, 300.
30. Araya, A.; Lowe, B. M. *Zeolites* **1984,** *4*, 280.
31. Engelhardt, G.; Michel, D. *High-resolution Solid-State NMR of Silicates and Zeolites;* Wiley, Chichester, 1987.
32. Barrer, R. M. *Hydrothermal Chemiwiy of Zeolites;* Academic Press: London, U. K., 1982; p 105.